VOL. 203, NO. 4 THE AMERICAN NATURALIST APRIL 2024

Intermittent Search, Not Strict Lévy Flight, Evolves under Relaxed Foraging Distribution Constraints

Winston Campeau,[1,*] **Andrew M. Simons,**[1] **and Brett Stevens**[2]

1. Department of Biology, Carleton University, Ottawa, Ontario K1S 5B6, Canada; 2. School of Mathematics and Statistics, Carleton University, Ottawa, Ontario K1S 5B6, Canada

Submitted July 6, 2023; Accepted November 9, 2023; Electronically published February 21, 2024

Online enhancements: supplemental PDF, videos S1–S3.

ABSTRACT: The survival of an animal depends on its success as a forager, and understanding the adaptations that result in successful foraging strategies is an enduring endeavour of behavioral ecology. Random walks are one of the primary mathematical descriptions of foraging behavior. Power law distributions are often used to model random walks, as they can characterize a wide range of behaviors, including Lévy walks. Empirical evidence indicates the prevalence and efficiency of Lévy walks as a foraging strategy, and theoretical work suggests an evolutionary origin. However, previous evolutionary models have assumed a priori that move lengths are drawn from a power law or other families of distributions. Here, we remove this restriction with a model that allows for the evolution of any distribution. Instead of Lévy walks, our model unfailingly results in the evolution of intermittent search, a random walk composed of two disjoint modes—frequent localized walks and infrequent extensive moves—that consistently outcompeted Lévy walks. We also demonstrate that foraging using intermittent search may resemble a Lévy walk because of interactions with the resources within an environment. These extrinsically generated Lévy-like walks belie an underlying behavior and may explain the prevalence of Lévy walks reported in the literature.

Keywords: evolutionary algorithm, optimal foraging, Lévy flight, intermittent search, random walks, search efficiency.

Introduction

An important component of an individual animal's fitness depends on the net energy gained through foraging, and the differential fitness of individual animals can depend on the variation among their foraging strategies; more efficient strategies result in more net energy gained, thereby increasing the probability of survival (Werner and Hall 1974; Krebs et al. 1977; Meire and Ervynck 1986). Thus, natural selection could favor those strategies that maximize net energy most efficiently. Random walks are often used to model different strategies of animal movement, with move lengths that vary according to an underlying probability distribution. Lévy flight, a type of random walk with move lengths distributed according to the power law $P(l) \sim l^{-u}$, where $1 < u < 3$, characterized by a mixture of frequent short steps and infrequent longer steps, has been argued to be a particularly efficient searching strategy (Viswanathan et al. 1999; Wosniack et al. 2017; Campeau et al. 2022) and is a searching behavior that has been observed among many organisms across multiple taxa (Sims et al. 2008, 2014, 2019; Humphries et al. 2010, 2012; Harris et al. 2012; Raichlen et al. 2014; Ariel et al. 2015; Kölzsch et al. 2015; Lihoreau et al. 2016; Reynolds et al. 2018; Reijers et al. 2019; Shirakawa et al. 2019). Specifically, the Lévy flight foraging hypothesis states that if the searcher has no memory and resources are scarce, revisitable, and information on their distribution is unknown to the forager, then a Lévy flight with exponent $u \simeq 2$ is an optimal or near-optimal searching strategy (Viswanathan et al. 2008).

The efficiency and adaptive potential of Lévy flight foraging has been substantiated by both empirical (Sims et al. 2008, 2019; Humphries et al. 2010, 2012; Lihoreau et al. 2016) and theoretical (Wosniack et al. 2017; Dannemann et al. 2018; Guinard and Korman 2021; Levernier et al. 2021; Campeau et al. 2022) evidence; thus, selection could favor Lévy-like behavior. However, there is an ongoing debate over the relative importance of Lévy-like behavior as a result of selection (the adaptationist or intrinsic hypothesis) or as an emergent property due to the features of the environment (the emergentist or extrinsic hypothesis). For example, spider monkeys (*Ateles geoffroyi*) exhibit emergent Lévy-like behavior in response to naturally occurring Lévy-like tree size distributions, utilizing mental maps (i.e., memory and perception) when

---

[*] Corresponding author; email: winston.campeau@carleton.ca.

ORCIDs: Campeau, https://orcid.org/0000-0001-6032-0186; Simons, https://orcid.org/0000-0002-0198-465X; Stevens, https://orcid.org/0000-0003-4336-1773.

American Naturalist, volume 203, number 4, April 2024. Published by The University of Chicago Press for The American Society of Naturalists. https://doi.org/10.1086/729220

determining which fruiting trees to visit (Boyer et al. 2006). In contrast, free-moving *Drosophila* larvae whose sensory neurons, supraesophageal ganglion, and brain synaptic activity were blocked exhibited intrinsically generated Lévy-like behavior (Sims et al. 2019). There is also evidence that some Lévy walks may simply be the by-product of crawling (such as the larvae from Sims et al. 2019) and are in fact Weierstrassian Lévy walks or stick-slip locomotion (Reynolds 2018, 2021). Whereas there is support for both the extrinsic and the intrinsic hypotheses and even mathematical proof for the optimality of Lévy walks (e.g., Guinard and Korman 2021), the intrinsic hypothesis suggests that natural selection favors Lévy-like behavior and poses the additional challenge of requiring evidence of ecological contexts driving its evolution through selection.

There are three notable lines of theoretical evidence that support an evolutionary origin for Lévy flight foraging. Wosniack et al. (2017) demonstrated that among the random walks governed by the power law exponents of $1 \leq u \leq 3$, ranging from ballistic ($u = 1$) to Lévy ($u = 2$) to Brownian motion ($u = 3$), a Lévy searching pattern was the most efficient over multiple distinct environments. Dannemann et al. (2018), using the same range of searching patterns, provided evidence that Lévy-like behavior can maximize the population abundance and minimize the extinctions of a predator-prey system. The combination of Wosniack's and Dannemann's research clearly evidence the advantages of Lévy-like behavior but not evolution through response to selection. One of the first models to demonstrate a response to selection used an evolutionary algorithm where the power law exponent u was modeled as a variable and heritable trait (Campeau et al. 2022). The results of the model corroborated both the advantages of Lévy-like behavior over different environments and its long-term stability while including both ecological and evolutionary contexts. Although evidence thus far supports the Lévy flight foraging hypothesis, its interpretation is limited by a common constraint; the a priori assumption that the searching patterns are governed by a power law. Greater insight into the evolution of foraging patterns requires a model that is free of such restrictions on the type of distribution on which natural selection acts. The de novo emergence of Lévy-like distributions would provide a more compelling case of an evolutionary origin.

Here, we use an evolutionary algorithm that includes several important evolutionary ecological contexts from previous models but dispenses with the a priori assumption of search patterns governed by a power law. In fact, our model makes no assumptions about any family of distributions. Furthermore, our model is meant to be rudimentary in that it isolates the effect of adaptations due to resource encounters and does not consider interesting extensions, such as mate and predator interactions or a limit to home range. Our model allows for the de novo evolution of search patterns with three possible interesting outcomes: (1) search patterns that approximate the resource distributions of the environment, (2) search patterns that approximate a Lévy-like distribution regardless of the resource distribution, and (3) novel search patterns that outcompete at least a Lévy walk. We encode a finite-size list of move lengths as a "pseudo-genome," where novel genomes are the result of recombination and a round of mutation. The shape of a genome's distribution of move lengths is therefore limited primarily by the size of the genome, thus allowing for a large solution space and providing firm theoretical grounds for not only testing the Lévy flight foraging hypothesis but the discovery of any optimal search pattern.

Material and Methods

We use an evolutionary algorithm to evolve optimal search patterns that may then be compared with existing hypotheses, such as the Lévy flight foraging hypothesis. From previous theoretical and mathematical models (Wosniack et al. 2017; Dannemann et al. 2018; Campeau et al. 2022) we include the ecological contexts of population size, life span, and a proxy for iteroparity (multiple matings over a lifetime), and we vary the environment using different Lévy dust (LD) distributions. We build on the previous evolutionary models by shifting variation from the level of a distribution parameter (the a priori assumption of selection acting on power law exponents; e.g., Wosniack et al. 2017; Campeau et al. 2022) to selection acting on the individual move lengths within a distribution to ask what distribution will result from selection. Evolutionary change in search patterns is driven by (1) the proportion of genetic material in subsequent generations determined by parent individuals' relative fitness, (2) a round of recombination, and (3) a round of mutation. Once a simulation has reached a point of equilibrium, we include an additional set of simulations to assay the fitness of the derived distributions under competition with ancestral and Lévy distributions, and we attempt to parameterize the derived distributions. We also discuss several modifications we have implemented to control for possible biases due to movement occurring on a lattice in the supplemental PDF.

Environments

A single environment is simulated as an $n \times n$ matrix, or lattice E, with resource entries $e_{i,j}$ and with periodic boundary conditions (i.e., the matrix is mapped onto a torus). Each environment is populated with a sequence of revisitable resources according to a LD distribution, a fractal distribution of resources. The first resource in the sequence is placed at random, with each subsequent resource placed at a distance of l away from the previous resource, where l is randomly selected from the probability mass function (pmf):

$$P(l) = \begin{cases} 0 & \text{if } l < 1 \text{ or } l > n/2, \\ l^{-u} & \text{if } 1 \leq l \leq n/2. \end{cases} \quad (1)$$

We chose $n/2$ as the point of truncation because $n/2$ is the maximum distance between any two points to travel in cardinal directions on a lattice with periodic boundary conditions. The direction of each resource placement in the sequence is selected at random from the set of all locations exactly l distance away. When a resource is placed, the value at the resultant location $e_{i,j}$ is incremented by 1. This process continues until the environment is populated with a sequence of $n^2 \cdot 10^{-3}$ resources, rounded down to the nearest integer. We chose random exponents $1 \leq u \leq 3$ as well as discrete values $u = 1, 2$, and 3 for our environments, as they represent the distinct distributions produced from ballistic, Lévy, and Brownian movement, respectively (fig. 1).

To increase the environmental variation individuals encounter and to approximate larger environments, we also utilized a type of procedural generation. A library of environments is produced for each generation of individuals, where each environment has the same amount of resources. Our simulations included libraries where the LD exponent is (1) fixed at $u = 1, 2$, or 3; (2) randomly varied between generations; or (3) randomly varied within each generation. An initial environment is selected at random for each individual. Then, on crossing the border of an environment, instead of appearing on the opposite side by periodic boundary conditions, a new environment is selected at random from the library and appended to the

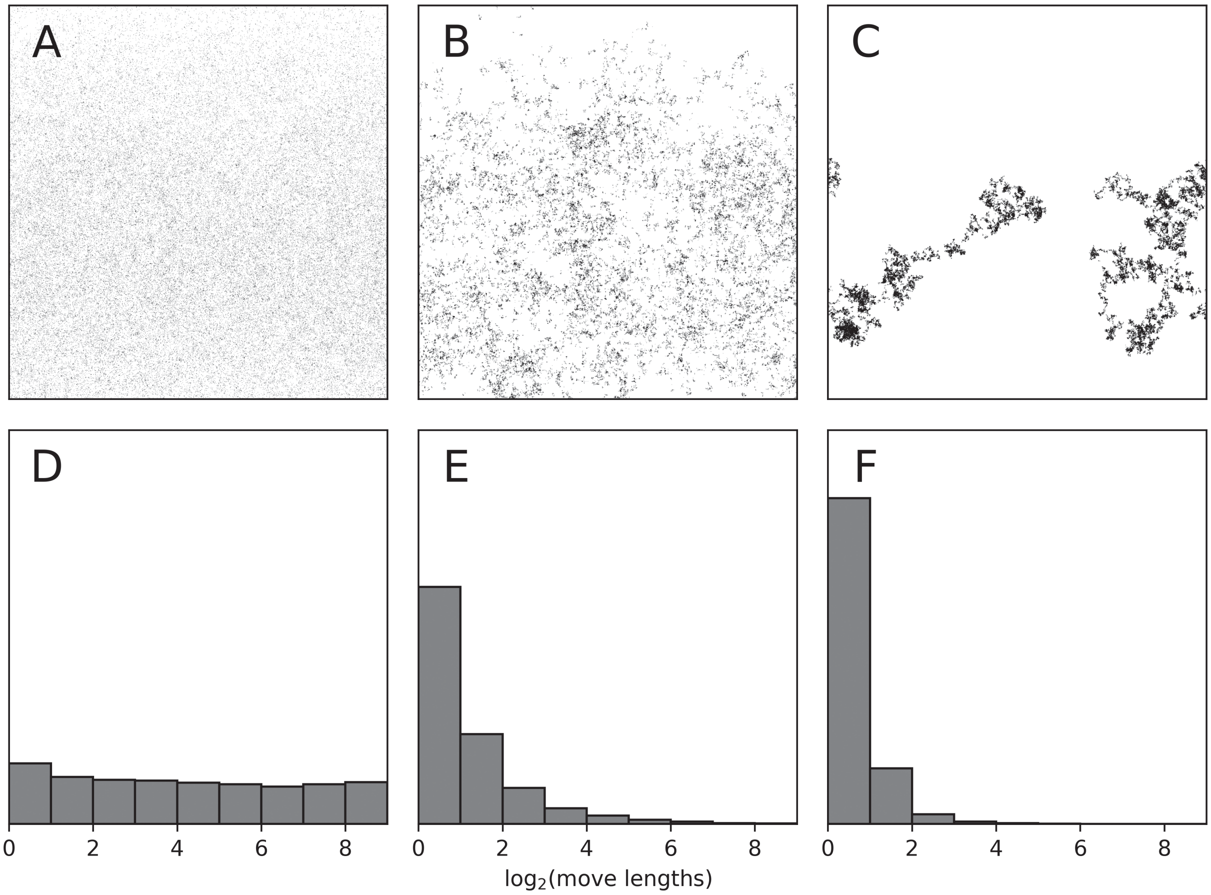

Figure 1: Examples of Lévy dust environments. *A–C*, $E_{997\times997}$ with $n^2 \cdot 10^{-1}$ (rounded down to the nearest integer) Lévy dust distributed resources with $u = 1, 2$, and 3, respectively. *D–F*, Histograms of the distributions used to produce *A–C*. We used 100-fold more resources than in our simulations to better illustrate the spatial nature of each exponent and log transformed the distributions to elucidate differences in shape; longer move lengths decrease in frequency with increasing u. Note that the y-axes of *D–F* are normalized frequencies.

border. See the supplemental PDF for more details on the procedurally generated environments.

Evolutionary Algorithm

An evolutionary algorithm is a population-based metaheuristic that borrows evolutionary mechanisms to approximate the solution to an optimization problem (Bäck and Schwefel 1993; Sloss and Gustafson 2020). An individual is a candidate solution to the optimization problem, and the quality of that solution is determined by a fitness function. The following sections will describe our definition of an individual (or candidate solution), the encoding of our evolutionary mechanisms (selection, reproduction, recombination, and mutation), and an outline of the main simulations and subsequent simulations of competition.

Definition of an Individual

An individual was encoded as the following list:

$$[G, pi, pj, \xi, \alpha\xi, \lambda, (I, J), \mathcal{D}],$$

where G contains the move lengths available to the individual, pi and pj store the position of the individual within an environment, ξ records the number of encountered resources, $\alpha\xi$ is the sum of ξ over time, λ is the life span, (I, J) stores the position of the current environment within a lattice of procedurally generated environments, and $\mathcal{D}$ is a growing dictionary that maps each (I, J) to an environment stored in the library of environments.

The term G is the pseudo-genome, a finite and unordered list of integer move lengths that can be initialized with any user-defined values. We propose two initial distributions that are interesting from an evolutionary perspective: random samples from a uniform distribution and an all-ones distribution (equivalent to Brownian motion). All move lengths are equally probable under a uniform distribution; thus, the amount of variation for selection to act on is maximized. Whereas the all-ones distribution is initially biased toward smaller move lengths and has an initial variance of zero, moving the minimal possible distance is perhaps the simplest initial searching behavior, barring no movement whatsoever. An individual's initial position (pi, pj) is random and is updated after every move. Individuals use a truncated random walk; each move is randomly selected from G, and movement occurs until either a resource is located or the full length of the move has been traveled. Movement occurs on a lattice, and the direction of each move length l is determined by randomly selecting an end point from the border of all locations exactly l distance away. An individual will move to the end point by taking random selections without replacement from a list of vertical and horizontal increments, continuing until the list is empty. See the supplemental PDF for additional details on the turning algorithm.

The range of perception of an individual is limited to its current cell, or location (i, j). In other words, the "resolution" of the simulation matches the perceptual capabilities of an individual and was chosen to intentionally minimize its information on the distribution of resources. When an individual encounters a resource at a location (i, j), ξ is incremented by $e_{i,j}$ (a growing sum), whereas $\alpha\xi$ is incremented by ξ after every entrywise move, regardless of resource encounter. Thus, ξ measures the total number of resources found, and $\alpha\xi$ is used to measure the average number of resources found over the life span of an individual. The life span of an individual λ is the total distance (or total time) available until that individual is removed from the simulation. We normalized life spans by the size of the environment according to $\varsigma \cdot n^2$; that is, each individual can theoretically visit every location of a single environment ς times (by default, $\varsigma = 20$). To track an individual's location within its procedurally generated environments, (I, J) is the index of its current environment, which is updated when crossing a boundary of its current environment and is stored as a key in a growing dictionary $\mathcal{D}$. Each key stored in the dictionary maps to an environment in the library of environments and preserves the relative locations of the procedurally generated environment for that individual. See the supplemental PDF for more details on the procedural generation of environments.

Selection or Fitness Function

Once all individuals have exhausted their life spans, their resultant average number of resources found over their life spans ($\alpha\xi$) are consigned to the fitness function. There is also the option to use the total number of resources located (ξ) as a measure of fitness, but we used $\alpha\xi$ for two reasons. The first is that ξ and $\alpha\xi$ are strongly correlated; thus, fitness differences are minimal (Campeau et al. 2022). The second is that the average energy over a life span $\alpha\xi$ would be markedly different for an individual that locates all of its resources at the beginning of its life span rather than at the end, but this would be indistinguishable using ξ, the energy at the end of a life span. Thus, ξ resembles semelparity because of a lifetime of energy invested into reproduction only at the end of a life span, whereas $\alpha\xi$ resembles a proxy for iteroparity because it considers the average amount of energy available over a life span and could be interpreted as the energy available for multiple rounds of reproduction. Organisms also more frequently evolve iteroparous reproduction strategies (Hughes 2017), and many semelparous strategies approximate iteroparity over shorter timescales (Hughes and Simons 2014); thus, $\alpha\xi$ is arguably the more appropriate choice.

The fitness function uses the $\alpha\xi$ values to determine the number of gametes that each parent will contribute to form the subsequent generation according to

$$\omega_i = \left\lceil \frac{K \cdot \alpha\xi_i}{\sum_{j=0}^{\psi} \alpha\xi_j} \right\rceil, \tag{2}$$

where for each parent, each half increment of ω_i represents one gamete, and the total number of gametes is based on the ratio of the carrying capacity (K) and their individual fitness relative to the sum of all surviving individuals (rounded up to the nearest integer). We index parents until ψ, instead of K, because an individual does not "survive" if its $\alpha\xi \leq 0$; thus, ψ is the number of surviving individuals. Each parent is assigned a value of ω_i, in descending order of $\alpha\xi$, until there are enough gametes to generate the next generation (i.e., $\sum \omega_i = K$). Therefore, although an individual may have the potential to have $\omega_i > 0$, there remains the possibility that its genetic information is not included in the reproductive pool. The resultant output is a list of pairs $(G_i, \omega_i) \in \Omega$, which is used to generate the next generation of individuals.

Reproduction through Recombination and Mutation

Mating is random, syngamous, and without incompatible mating types. Two parent pairs, (G_i, ω_i) and (G_j, ω_j), are randomly selected from Ω, and on selection each parental genome (G_i and G_j) is first randomly rearranged (i.e., no linkage). One-half of each parental genome is then assigned at random as its gametic contribution to the single offspring, G_k (fig. 2). Accordingly, ω_i and ω_j are then decremented by one-half. Whereas we recognize the differential energetic burdens of reproduction and its evolutionary importance, we believe its inclusion would add unnecessary complexity in the scope of this article.

The resultant offspring genome then undergoes a round of mutation. First, a fixed number of move lengths are randomly selected for mutation. Each move length is then modified by a random value m, from a scaled and discretized unit normal distribution. We discretize by rounding to comply with the integer requirement and use a scalar, η, to vary the magnitude of mutation. We extend the same bound restrictions from equation (1), such that a mutated move length cannot go below 1 and cannot exceed $n/2$. Mutations resulting in move lengths below 1 or above $n/2$ will roll back into the space of $1 \leq l \leq n/2$, where the amount of rollback is the difference over the bound. For example, if $n/2 = 100$, then $l = 110$ would become $l = 90$ and $l = -10$ would become $l = 11$. The value of η should be carefully selected as to not result in mutations so large that the resultant move lengths bounce over the bounds until reaching an equilibrium ($5\eta < n/2$ is a sufficient condition to avoid this behavior). The process of reproduction, recombination, and mutation continues until all $\omega_i = 0$. In the case where there is only one parent remaining, reproduction switches to asexual, and the offspring genome is a mutated copy of the parent genome.

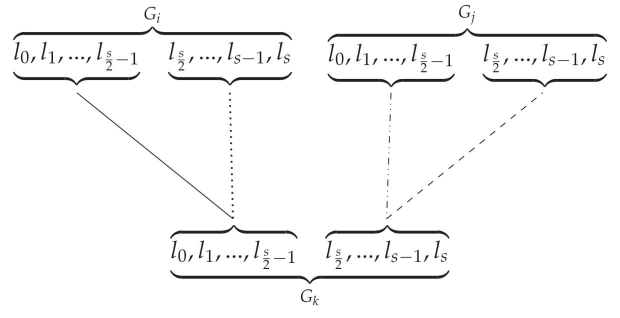

Figure 2: Modeled assortment and syngamous offspring production. Following selection (see text), one of two halves of each randomly rearranged parental genomes (G, a finite, unordered list of move lengths l) is assigned through independent assortment as the gamete to form one of four possible offspring genomes (indicated by the dashed, dotted, solid, and dashed-dotted lines). An offspring's genome is thus composed of a random sample of move lengths inherited equally from both selected parental genomes.

Simulation Framework

The simulation is initialized by choosing an exponent(s) for the distribution of resources, the maximum number of generations, the mutation rate and magnitude, the size of the environment and the library that contains them, and the size of the population and their genomes. The library of environments is generated first, with each environment receiving $n^2 \cdot 10^{-3}$ resources, rounded down to the nearest integer. Next, the starting population is generated, with a specified initial distribution for G: all-ones or random uniform move lengths for this study. The individuals traverse procedurally generated environments until all of their life spans are exhausted. The population is then assessed by the fitness function, and the offspring are generated by the recombination and mutation of random selections from any two parents that were admitted to the reproductive pool. This process continues until the number of offspring is equal to the selected population size. The offspring become the subsequent population, and the process is repeated until either the mean population $\alpha\xi$ stabilizes or the total number of generations is exhausted (10^4 by default).

All genomes are saved every gth generation (by default, $g = 1$) as a "fossil record," similar to the fossil record in Lenski's long-term evolution experiment (Wiser and Lenski 2015), allowing the simulation to be restarted at any point, if necessary. These data also allow for competitive fitness assays between our ancestral and derived foraging patterns as well as assays of the derived foraging patterns competing with Lévy foraging patterns, to determine quantitative differences and provide qualitative insight. For the competition simulations, the initial population was composed of either derived and ancestral individuals or derived and Lévy individuals, in equal frequency. In these competition assays, reproduction was strictly asexual; parents produced offspring with exact copies of their genomes. Last, the two populations competed for a fraction of a carrying capacity, and a simulation was stopped once an equilibrium was reached (i.e., only one type remained).

Simulations and results were programmed using Python 3.10.6 and the numpy (Harris et al. 2020), scipy (Virtanen et al. 2020), pandas (McKinney 2010), multiprocessing (McKerns et al. 2012), and Matplotlib (Caswell et al. 2021) libraries in addition to the Python standard library. Computations were performed on the Graham, Cedar, Narval, and Niagara supercomputers at the Digital Research Alliance of Canada (Loken et al. 2010; Ponce et al. 2019).

Distribution Characterization

Our evolutionary algorithm constrains the evolution of distributions to containing s move lengths (the total number of move lengths in G), where each move length cannot exceed a value of $n/2$. This means that our algorithm can result in a potential

$$\binom{\frac{n}{2} + s - 1}{s}$$

unique distributions. For example, $s = 100$ and $n/2 = 100$ is approximately $4.5 \cdot 10^{58}$ possibilities, and, albeit not without many correlated distributions, it is difficult to anticipate exactly what methods would be necessary to characterize the derived distributions (i.e., there is no guarantee whether distribution fitting will be informative). Based on visual inspection of the derived distributions and their behavior, we considered comparisons with an array of candidate models of random walks (e.g., composite random walks or power laws) and measured their scaling exponents by their mean-squared displacement (MSD).

Results

We ran simulations where populations of 100 individuals would search for revisitable resources within a procedurally generated environment. Their initial environment was encoded as a matrix $E_{n\times n}$, with dimension $n = 997$ (see the supplemental PDF for why n is prime). Each matrix had resources distributed by either successive ballistic, Lévy, or Brownian flights (fig. 1) or mixtures of resource distributions with random LD exponents. Simulating evolution over these distinct distributions enabled us to test whether the derived distributions would converge to environmental, Lévy-like, or novel distributions. Each individual was assigned a life span of $\lambda = 20 \cdot n^2$ steps and an initial G composed of either 200 random uniform move lengths $1 \leq l \leq n/2$ or 200 ones. We ran simulations with each initial G for the environments with discrete LD exponents and with only the random uniform G for environments with randomly varied LD exponents between and within generations. We ran replications for only the random uniform starting G, thus resulting in a total of 13 evolutionary simulations. We set a fixed mutation rate such that 12 out of 200 move lengths were always admitted for mutation, with magnitude $\eta = 2$. Once the evolution of G stabilized, we then competed the derived distributions against ancestral distributions to test for adaptive evolution and against Lévy distributions to determine quantitative and qualitative differences, if any.

Distribution Evolution and Characterization

All simulations resulted in similar derived distributions, regardless of their environment (fig. 3; videos S1, S2; videos S1–S3 are available online). The random uniform and all-ones starting conditions required approximately 400 and 5,000 generations to reach equilibration, respectively. The derived distributions are bimodal with the primary mode clustered near 1 and a secondary mode clustered on the $n/2$ point of truncation. The resultant behavior of the bimodal distributions is an emergent two-phase walk (fig. 4*C*–4*E*; video S3*A*). The primary phase is highly localized and visually similar to a Brownian walk. The secondary phase could be described as a ballistic or scaled Brownian walk, where the most common move length was $l \approx n/2$, constituting ≈17% of 18 unique values, although the size of the secondary modes (2.5 move lengths on average) were too small for distribution fitting. From the noncontinuity of the derived distributions and visual inspection, we proposed two candidate composite random walks:

$$\begin{aligned} p(l) = {} & p_{\text{primary}}((1 - p_{\text{geometric}})^{l-1} p_{\text{geometric}}) \\ & + (1 - p_{\text{primary}})(n/2), \end{aligned} \tag{3}$$

$$\begin{aligned} p(l) = {} & p_{\text{primary}}(l^{-u}) + (1 - p_{\text{primary}})(n/2), \\ & 1 \leq u \leq 5, \end{aligned} \tag{4}$$

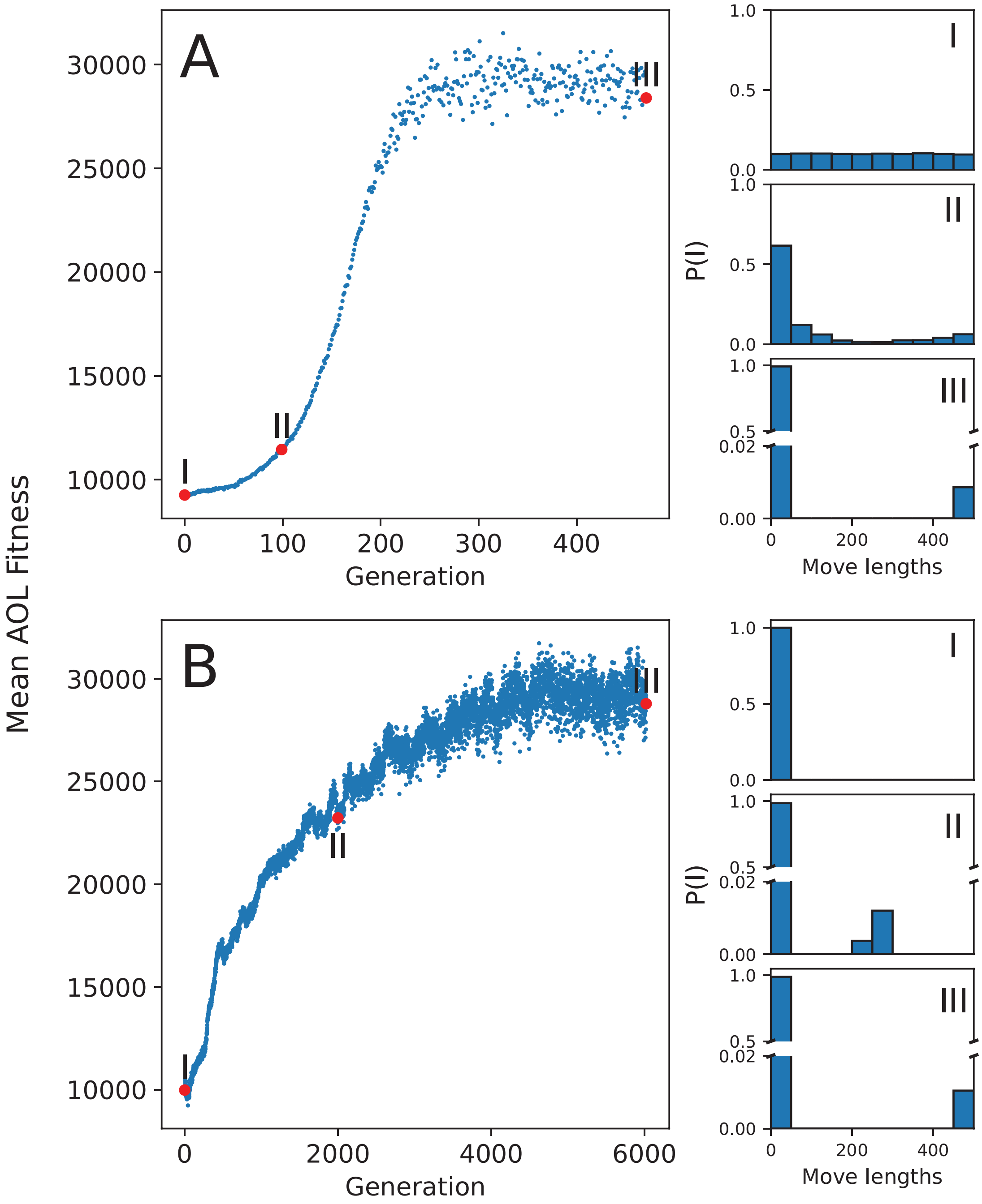

Figure 3: Evolution of foraging behavior in response to Lévy dust $u = 2.0$ resources (fig. 1*B*). The labeled red points highlight changes in the move-length distributions over generational time. *A* shows the change in mean fitness (AOL = average number of resources found over a life span) starting from a uniform distribution. *A-I*, *A-II*, and *A-III* are frequency plots of the ancestral and derived distributions corresponding with the labeled points in *A*, occurring at the 0th, 100th, and final generation. *B* shows the change in mean fitness starting from an all-ones distribution. *B-I*, *BI-I*, and *B-III* are frequency plots of the ancestral and derived distributions corresponding with the labeled points in *B*, occurring at the 0th, 2,000th, and final generation. The *y*-axis breaks in *A-III*, *B-II*, and *B-III* highlight the secondary mode of the distributions.

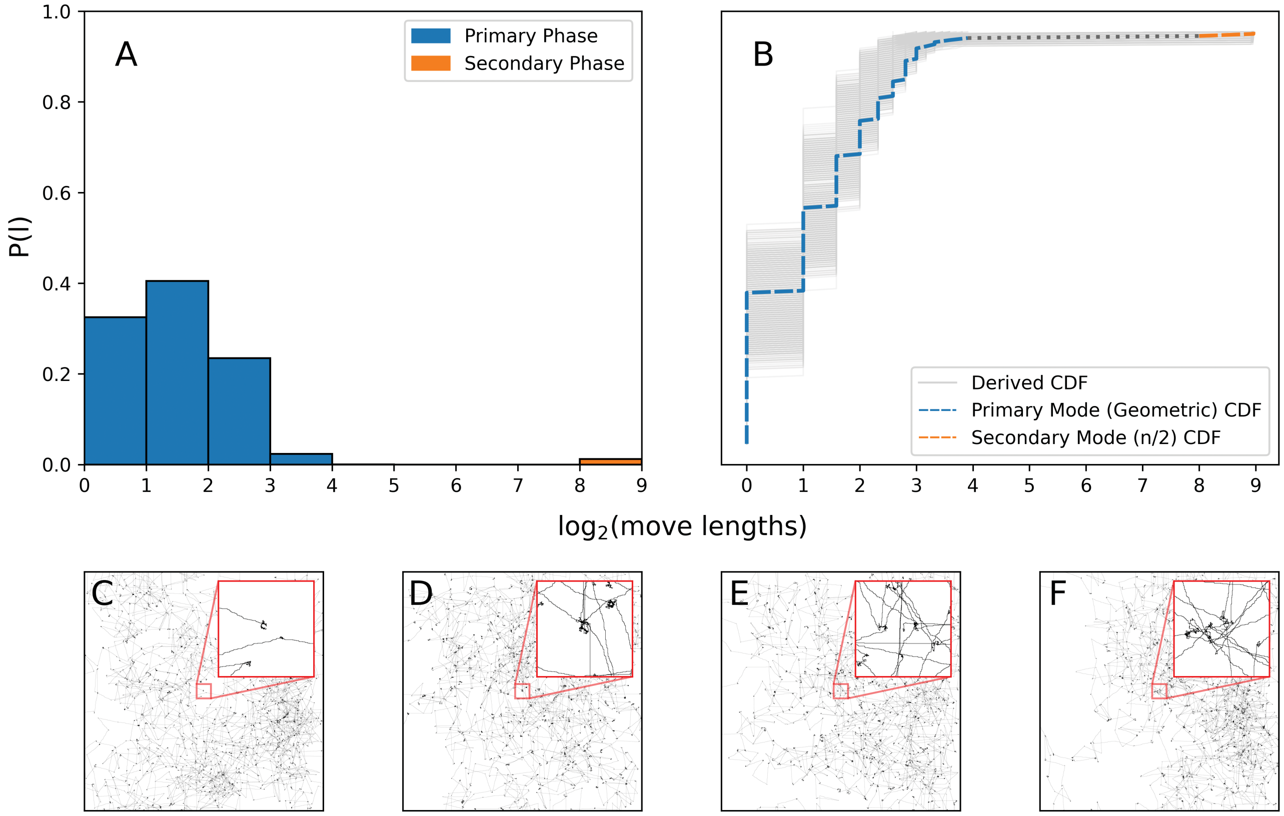

Figure 4: Geometric distribution–based model fitted to the derived distributions. *A* is the move-length probability distribution averaged over all individuals. *B* contains the superimposed cumulative distribution function (CDF) of each individual in comparison to the best-fit CDF obtained from equation (3) with $p_{\text{primary}} = 0.9875$ and $p_{\text{geometric}} = 0.33$. *C–E* show walks derived from Lévy dust environments with $u = 1$, 2, and 3, respectively, whereas *F* shows a walk from the model of best fit.

where p_{primary} is the probability of drawing a move length from the primary mode, modeled by either a geometric distribution (the discrete equivalent of an exponential distribution) with $p_{\text{geometric}}$ or a power law with $1 \leq u \leq 5$, and a $1 - p_{\text{primary}}$ probability of drawing from the secondary mode, which is simply a move length of $l = n/2$. To determine the suitability of each model, we first isolated the primary modes from each of our 1,300 derived distributions and compared their cumulative distribution functions over an array of 10^3 power law exponents u from $[1.0, 5.0]$ and $p_{\text{geometric}}$ from $[0, 1]$ using k-sample Anderson-Darling (AD) tests. The null hypothesis of the k-sample AD test is that two (or more) samples are drawn from the same distribution; a power law with $u \approx 1.9$ resulted in a failure to reject the null hypothesis for ≈1% of the comparisons, whereas a geometric distribution with $p_{\text{geometric}} \approx 0.33$ resulted in a failure to reject the null hypothesis for ≈58% of the comparisons. Randomly adding either two or three move lengths of $l = n/2$ to the optimal geometric distribution resulted in a failure to reject the null for ≈60% of the comparisons with the complete derived distributions. The behavior of the resultant model was then visually compared with a distribution derived from each environment (fig. 4; video S3*A*, S3*B*).

Next, we computed the scaling exponent of one of the derived populations and included a Lévy walk (as defined by the pmf in eq. [1]) for comparison. The scaling exponent is obtained by measuring the displacement of multiple individuals over increasing periods of time, taking the mean of their squared displacements and observing how those MSDs change over time (i.e., measuring the slope). The scaling exponent can be used to compare and characterize the exploratory behavior of different random walks (Einstein 1905; Frenkel and Smit 2023). A simple Brownian walk has a scaling exponent of $\alpha = 1$, indicating a walk that displaces linearly in time, whereas the scaling exponents for the Lévy walks and derived walks, computed using a least squares Levenberg-Marquardt algorithm based on the statistical regularity of the data and its use for similar analysis (Zhou et al. 2018; Liu et al. 2021), were found to be $\alpha = 1.97$ ($R^2 = 0.999$) and $\alpha = 1.997$ ($R^2 = 0.999$), respectively (fig. S1; figs S1–S5 are available online). These values indicate that individuals using either strategy will explore the environment much faster than a Brownian walk and that the derived walks will do so marginally faster than Lévy walks but are otherwise difficult to distinguish by their scaling exponents alone.

Last, we performed an exploratory analysis to examine the "realized" distributions of move lengths. We define a realized distribution as the result of the truncated move lengths, rather than the lengths pulled from a distribution. For example, an individual might pull $l = 498$ from its distribution but encounter a resource after only 10 steps; thus, the realized length is the truncated length of 10 steps. We collected the realized distributions from each type of environment over a range of resource densities (the tested $n^2 \cdot 10^{-3}$ and one fold up and down) and a life span of $\lambda = n^2$ (the minimum to span the entire environment) to determine how they might differ from the derived distributions. The distributions of realized move lengths were increasingly contiguous with increasing resource density and decreasing resource clumpiness (i.e., $u < 3$; fig. 5). We also measured the degree of contiguousness by sorting the realized distributions in increasing order and measuring the largest gap (any difference greater than 1 between successive move lengths). Whereas the largest gap of the derived distributions tended toward $(n/2) - 1$, the realized distributions were either contiguous or had gaps no larger than size 4. Assuming a power law fit almost always resulted in exponents falling in the Lévy-like range, with $1 < u < 3$, often close to a "true" Lévy walk of $u = 2.0$ (fig. S2).

Competition Simulations

We computed a sum total of 324 competition simulations between the derived distributions and either a Lévy walk with $u = 2.0$ or root and midgeneration ancestors from the simulated fossil records. Competition between derived and Lévy occurred over environments LD = 1.0, 2.0, and 3.0 with either $n^2 \cdot 10^{-3}$ or $n^2 \cdot 10^{-4}$ resources, with life spans of $\lambda = 20 \cdot n^2$ or $\lambda = n^2$, starting with populations of either 10 or 100 each (i.e., competing for carrying capacities of either 20 or 200) and with the Lévy walks having access to a G of size 200 or 2,000. Three replicates were computed for each of these 48 possible combinations, therefore totaling 144 simulations for a single population of derived distributions. The derived populations from our six evolutionary simulations were near indistinguishable, so we replicated the competition simulations using only two of the derived populations: individuals evolved from all-ones distributions and LD $u = 2.0$ and random uniform distributions and LD $u = 1.0$, thus totaling 288 simulations. We competed the derived distributions against their root ancestor (i.e., the first generation) and a midgeneration distribution (100th for the random uniform case and 2,000th for all-ones), under the same conditions in which they evolved and with three replicates each, totaling 36 simulations.

The derived populations won 100% of the 324 competition simulations. The median number of generations required to displace the Lévy populations across all simulations was two. The largest sources of variance in generational time among the simulations were life span and the derived population (fig. 6). Life spans of $\lambda = 20 \cdot n^2$ required a median of two generations (min = 1, max = 3), whereas $\lambda = n^2$ took three generations (min = 1, max = 11). Within the life span of $\lambda = 20 \cdot n^2$, the initial all-ones distribution required a median of two generations (min = 1, max = 3), whereas the initial random uniform distributions required one (min = 1, max = 2), and within the life span of $\lambda = n^2$ the initial all-ones distributions required a median of four generations (min = 1, max = 11), whereas the initial random uniform distributions required three (min = 1, max = 6). We also include a subset of simulations using very small life spans $\lambda = 0.1 \cdot n^2$, available in the supplemental PDF. The overall median number of generations required to displace the ancestral populations was two (min = 1, max = 2). Although the derived distributions were largely indistinguishable, the differences in generational time among the two starting conditions to displace the Lévy populations motivated an additional set of analyses and simulation to explain those differences, and these results are available in the supplemental PDF.

In a final, and additional, set of simulations we assayed the success of the derived populations against Lévy populations scaled with n. We scaled the environment up and down by a factor of two ($2n = 1{,}994$ and $n/2 = 498$) and set life span $\lambda = 20 \cdot n^2$, patch density $10^{-3} \cdot n^2$, and a G of size 2,000 for the Lévy individuals, and over each environment type, with three replications. We adjusted the derived distributions by simply scaling only the secondary mode by the same factor of two. The scaled derived distributions won 100% of these 18 additional simulations. The median number of generations required to displace the Lévy distributions was two (min = 2, max = 2) in the upscaled environments and three (min = 2, max = 3) in the downscaled environments.

Discussion

The Lévy flight foraging hypothesis, in its simplest form, is the claim that because Lévy flight is an optimal or at least adaptive searching strategy, then natural selection should result in Lévy-like behavior. Empirical evidence has indicated that many organisms exhibit Lévy-like

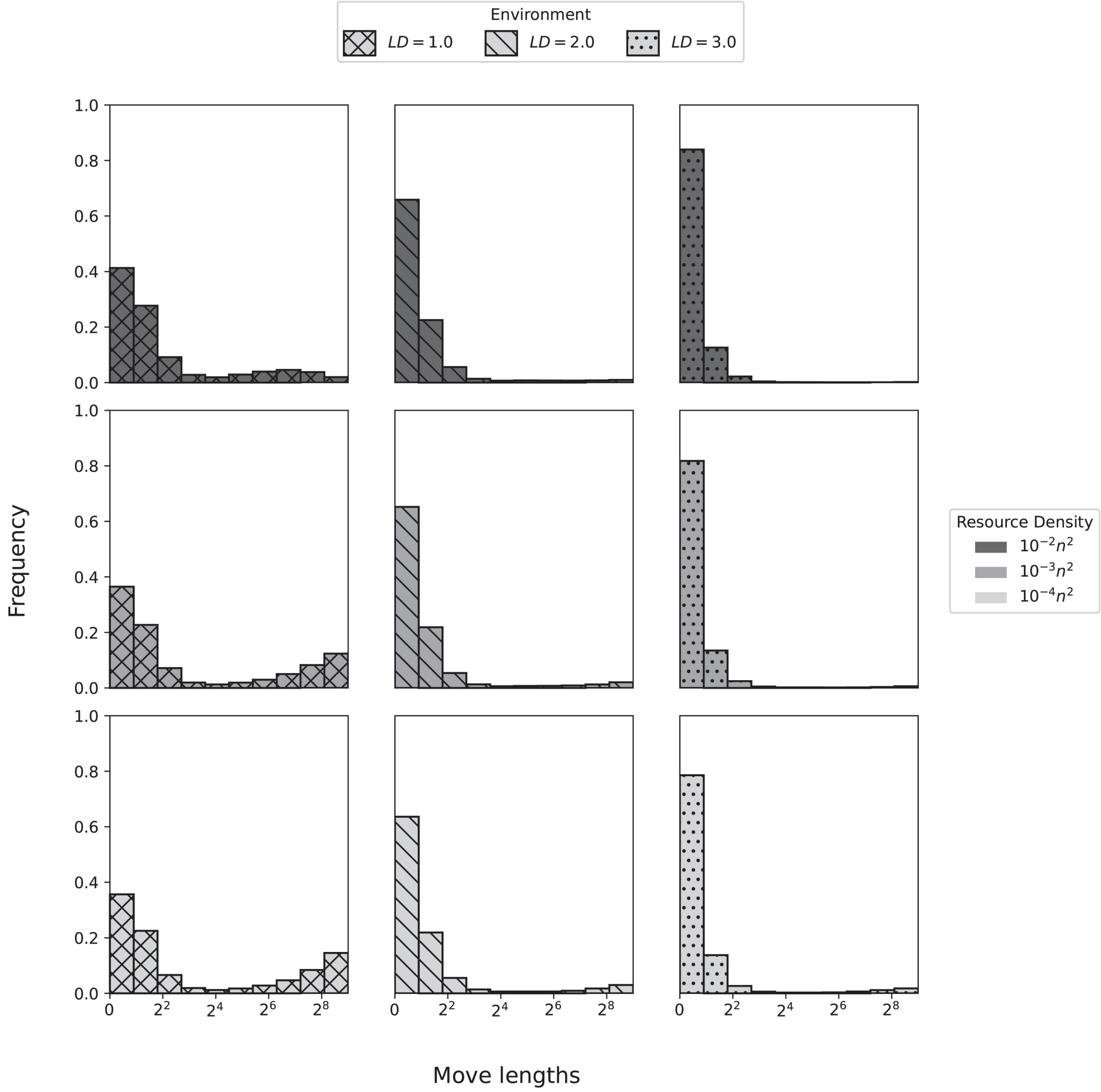

Figure 5: Impact of resource density and distribution on the distribution of realized move lengths pulled from a fixed derived distribution shown in figure 3*A-III*. Shown are realized distributions of move lengths over each tested environment—ballistic ($u = 1.0$), Lévy ($u = 2.0$), and Brownian ($u = 3.0$) distributed resources—and with the tested density of $10^{-3} \cdot n^2$ resources in addition to a 10-fold factor above and below. Each distribution was generated from the truncated moves of five walks, each with life span $\lambda = n^2$ steps. Note that move lengths are on a logarithmic scale.

behavior, but whether that behavior is intrinsic and the result of natural selection, is extrinsic and an emergent phenomenon due to interactions with the environment, or a mixture of both is unclear. Lévy walks have been evidenced as adaptive over various environments (Wosniack et al. 2017), a strategy that increases the stability of Lotka-Volterra systems (Dannemann et al. 2018), and as a response to selection regardless of the fractal dimension of resources and under several evolutionary and ecological contexts (Campeau et al. 2022). However, a common

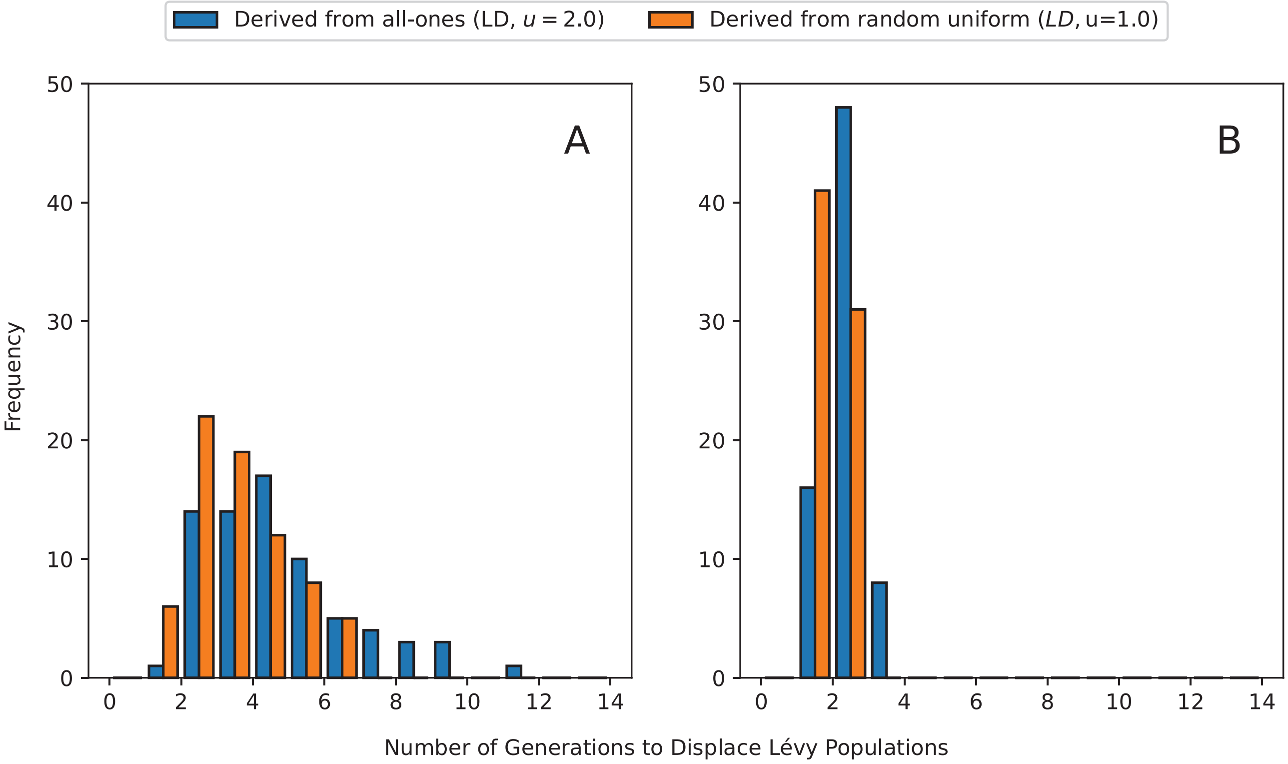

Figure 6: Number of generations required for the derived populations to displace the Lévy populations from the competition simulations. *A* is life spans $\lambda = n^2$, and *B* is life spans $\lambda = 20 \cdot n^2$. LD = Lévy dust.

limitation of these studies is the a priori assumption that foragers adhere to search patterns governed by power laws. Building on existing models, we removed this limitation and constructed an evolutionary algorithm that allowed for the de novo evolution of search patterns; we shifted the resolution on which evolutionary mechanisms could act on from the parameters of a distribution to the distributions themselves. We proposed three possible interesting outcomes: (1) the patterns approximate their environment, (2) the patterns converge to Lévy-like distributions, or (3) the search patterns are novel and also outcompete at least a Lévy walk. Our results unequivocally point to the third outcome.

The search patterns of our derived populations, regardless of their initial conditions, all converged to a search composed of two emergent phases, a long and highly localized phase and a shorter ballistic phase, where under competition they outcompeted Lévy walks, including in scaled environments. This search pattern is not new to the literature and is commonly referred to as intermittent search (Bénichou et al. 2005, 2011; Bénichou et al. 2006), a composite random walk that is known to outcompete Lévy-like behavior (Benhamou and Collet 2015) and characterizes the behavior of some organisms (Reynolds and Frye 2007). The advantage of intermittent search should feel intuitive; when searching for food (e.g., mushrooms) or something lost, humans will sometimes search a small area intensively before eventually giving up and switching to a new location (Pacheco-Cobos et al. 2019). The primary mode of the derived distributions, composed of smaller moves, provides the capability to search intensively and exploit clustered resources. The secondary mode, composed of a few large moves, allows an individual to quickly explore the environment before eventually encountering another resource. We also conjecture that limiting the size of the larger moves may be unnecessary. For example, it may be sufficient to simply continue walking until a resource is located, which does not require a predetermined distance but accomplishes the same result.

A similar search, area-restricted search (Kareiva and Odell 1987; Dorfman et al. 2022), can be characterized by an intermittent search as foragers switch between an intense localized search and an exploratory global phase. The primary difference between the two strategies is that turning angles increase following resource encounters under an area-restricted search—our evolved walks do not react in response to resource encounters, they are simply random draws from a single distribution. Evolutionary algorithms and models of reinforcement learning have previously been used to evidence the adaptive value of area-restricted search, but these models either acted primarily on the duration spent in the local search and the directionality of the local and global phases (therefore presupposing the option of intermittent search; Hills 2006; Scharf et al. 2009) or included an explicit capability to learn (López-Incera et al. 2020). In contrast, our derived distributions are the result of combinatorial optimization from random processes in the absence of sensory or memory effects; each distribution G is a multiset of size 200, with move lengths belonging to a finite set of size 498 (the restriction set by eq. [1]); thus, there were a possible 697!/(200!497!) unique distributions, more than the sum of both the legal and theoretical number of positions in the game Go (Tromp 2016; Walraet and Tromp 2016). Furthermore, we utilized a form of procedurally generated environments, whose increased environmental variation decreased the risk of artifacts that might incur from a single environment with periodic boundary conditions. Thus, the consistent result of intermittent search in all of our simulations is a strong indication of the selective advantage of intermittent search as an intrinsically generated behavior.

If intermittent search is intrinsically generated, then its behavior may only ever be observed within a vacuum and may be mistaken for Lévy-like behavior, since interactions with the environment will inevitably affect the observed searching behavior. For example, "brain-blocked" free-moving *Drosophila* larvae exhibited movement similar to a Lévy walk with an power law exponent of 1.96 (Sims et al. 2019). By eliminating the larvae's sensory information of the environment, an alluring hypothesis is that their movement was an intrinsically generated Lévy walk. However, the larvae could collide with one another and the edges of their arena, and the agar coating the arena may have not been featureless. We demonstrated this possibility by allowing the derived individuals to search within environments with various distributions and densities of resources and collecting the "realized" move lengths (fig. 5). Whereas the evolved distributions were bimodal and disjoint, the observed distributions were contiguous, heavy tailed, and under the assumption of a power law exhibited exponents that fell within the range of Lévy-like behavior, $1 < u < 3$ (fig. S2). The MSD scaling exponent of the derived behavior, $\alpha = 1.997$, was nearly identical to that of a Lévy walk, $\alpha = 1.97$, and scaling exponents have been reported in the literature as evidence to characterize organisms as using a Lévy walk, with many $1.6 \leq \alpha \leq 1.9$ (Ramos-Fernandez et al. 2004; Miramontes et al. 2014; Ariel et al. 2015; Murakami et al. 2015), further conflating the two behaviors. The scaling exponent of our derived individuals is also a near exact match with the results of the model from López-Incera et al. (2020), despite our unique assumptions.

Although our results strongly indicate the adaptiveness of intermittent search, we recognize that our model is chasing after an optimal and potentially universal strategy that may not exist. Selection acts on preexisting variation, and intermittent search may be unattainable or costly to evolve in real-life organisms, despite its advantages. Thus, we do not necessarily expect intrinsically generated intermittent search (or any other distribution generated by our model) to be a universally available strategy. However, with the appropriate ecological contexts and given the evolutionary nature of the model's heuristics, we believe our model has the potential to reveal a class of biologically relevant and intrinsically generated search patterns, one that includes intermittent search.

Conclusion

We overcame the a priori constraint of searching behavior governed by power laws and constructed a model that allowed for the evolution of virtually any probability distribution. Whereas the Lévy flight foraging hypothesis predicts the evolution of adaptations for Lévy-like behavior, our model instead resulted in intermittent search, a behavior that characterizes an area-restricted search. Our results do not eliminate the possibility of intrinsically generated Lévy-like behavior, but they do evidence the optimality of an intrinsically generated intermittent searching behavior—a behavior that outcompeted Lévy walks in all 324 of our tested instances, most often requiring only two generations. We also demonstrated that intermittent search could be perceived as Lévy-like behavior due to interactions with the environment, thus supporting aspects of the extrinsic hypothesis. The results of our model could be confirmed with experiments that minimize or eliminate truncated movement due to interactions with the environment. Furthermore, if intermittent search is intrinsically generated, then the Fourier analysis of neuronal activity in, say, peristaltic-driven motion (e.g., pedal waves in larvae, as described by Reynolds [2021]) might reveal two primary oscillatory components: a low-frequency and large-amplitude component and a high-frequency and low-amplitude component that accounts for the majority of the power spectrum. Our model, as presented here, is most appropriate for exploring the evolution of intrinsically generated behavior, specifically in the absence of information on the environment. The model could be extended by subjecting the distribution of turning angles to selection or including aspects of memory (working memory, as opposed to a genetic memory) to explore more complex behaviors. For example, turning angles are not independent of resource encounters under area-restricted search (Dorfman et al. 2022), and selection could act on the correlation of turning angles and resource encounters. The evolutionary mechanisms could include saltatory mutations (i.e., mutation probabilities other than normal) and considerations for the relatedness of individuals to alter how the algorithm explores the solution space. The model could also include predator and mate encounters to determine how combinations of encounters affect the evolution of individual walks. The environments could include spatiotemporal fluctuations in resource density to assess how food availability alters searching behavior. Last, our model could include costs for cognitive or physiological adaptations and explore how those costs might affect the evolution of intermittent search or whichever resultant evolved walks. We hope the results presented here will encourage further research on the potential evolutionary origins of an intrinsic and intermittent search.

Acknowledgments

Thanks to R. Taylor for providing additional computational resources; to F. Lutscher and R. Gorelick for their insight and advice; to A. Cheslock, I. Berberi, and M. Coffey for their support; and to the editors and referees for their detailed and helpful suggestions. This work was supported by the Natural Sciences and Engineering Research Council of Canada (RGPIN-2021-03832 [A.M.S.], RGPIN-2017-06392 [B.S.]).

Statement of Authorship

All authors contributed to the original conception of the model and to the development of the experimental methods. W.C. wrote the original draft, coded the simulations, and collected, analyzed, validated, and prepared visualizations of the resultant data. All authors reviewed and edited the writing at all stages of revision.

Data and Code Availability

All data and code have been deposited in the Zenodo data repository (https://zenodo.org/doi/10.5281/zenodo.7971749; Campeau et al. 2023).

Literature Cited

Ariel, G., A. Rabani, S. Benisty, J. D. Partridge, R. M. Harshey, and A. Be'er. 2015. Swarming bacteria migrate by Lévy walk. Nature Communications 6:8396.

Bäck, T., and H.-P. Schwefel. 1993. An overview of evolutionary algorithms for parameter optimization. Evolutionary Computation 1:1–23.

Benhamou, S., and J. Collet. 2015. Ultimate failure of the Lévy foraging hypothesis: two-scale searching strategies outperform scale-free ones even when prey are scarce and cryptic. Journal of Theoretical Biology 387:221–227.

Bénichou, O., M. Coppey, M. Moreau, P.-H. Suet, and R. Voituriez. 2005. Optimal search strategies for hidden targets. Physical Review Letters 94:198101.

Bénichou, O., M. Coppey, M. Moreau, and R. Voituriez. 2006. Intermittent search strategies: when losing time becomes efficient. Europhysics Letters 75:349.

Bénichou, O., C. Loverdo, M. Moreau, and R. Voituriez. 2011. Intermittent search strategies. Reviews of Modern Physics 83:81–129.

Boyer, D., G. Ramos-Fernandez, O. Miramontes, J. Mateos, C. Germinal, H. Larralde, H. Ramos, and F. Rojas. 2006. Scale-free foraging by primates emerges from their interaction with a complex environment. Proceedings of the Royal Society B 273:1743–1750.

Campeau, W., A. M. Simons, and B. Stevens. 2022. The evolutionary maintenance of Lévy flight foraging. PLoS Computational Biology 18:e1009490.

———. 2023. Data from: Intermittent search, not strict Lévy flight, evolves under relaxed foraging distribution constraints. American Naturalist, Zenodo, https://zenodo.org/doi/10.5281/zenodo.7971749.

Caswell, T. A., M. Droettboom, A. Lee, d. E. S. Andrade, J. Hunter, T. Hoffmann, E. Firing, et al. 2021. matplotlib/matplotlib: REL: v3.4.0rc3. Zenodo, https://doi.org/10.5281/zenodo.4595937.

Dannemann, T., D. Boyer, and O. Miramontes. 2018. Lévy flight movements prevent extinctions and maximize population abundances in fragile Lotka-Volterra systems. Proceedings of the National Academy of Sciences of the USA 115:3794–3799.

Dorfman, A., T. T. Hills, and I. Scharf. 2022. A guide to area-restricted search: a foundational foraging behaviour. Biological Reviews 97:2076–2089.

Einstein, A. 1905. About the movement of suspended particles in liquids at rest as required by the molecular kinetic theory of heat [Über die von der molekularkinetischen Theorie der Wärme geforderte Bewegung von in ruhenden Flüssigkeiten suspendierten Teilchen]. Annalen der Physik 322:549–560.

Frenkel, D., and B. Smit. 2023. Understanding molecular simulation: from algorithms to applications. Elsevier Science, Amsterdam.

Guinard, B., and A. Korman. 2021. Intermittent inverse-square Lévy walks are optimal for finding targets of all sizes. Science Advances 7:eabe8211.

Harris, C. R., K. J. Millman, S. J. van der Walt, R. Gommers, P. Virtanen, D. Cournapeau, E. Wieser, et al. 2020. Array programming with numpy. Nature 585:357–362.

Harris, T. H., E. J. Banigan, D. A. Christian, C. Konradt, E. D. Tait Wojno, K. Norose, E. H. Wilson, et al. 2012. Generalized Lévy walks and the role of chemokines in migration of effector CD8$^+$ T cells. Nature 486:545–548.

Hills, T. T. 2006. Animal foraging and the evolution of goal-directed cognition. Cognitive Science 30:3–41.

Hughes, P. W. 2017. Between semelparity and iteroparity: empirical evidence for a continuum of modes of parity. Ecology and Evolution 7:8232–8261.

Hughes, P. W., and A. M. Simons. 2014. The continuum between semelparity and iteroparity: plastic expression of parity in response to season length manipulation in *Lobelia inflata*. BMC Evolutionary Biology 14:90.

Humphries, N. E., N. Queiroz, J. R. M. Dyer, N. G. Pade, M. K. Musyl, K. M. Schaefer, D. W. Fuller, et al. 2010. Environmental context explains Lévy and Brownian movement patterns of marine predators. Nature 465:1066–1069.

Humphries, N. E., H. Weimerskirch, N. Queiroz, E. J. Southall, and D. W. Sims. 2012. Foraging success of biological Lévy flights recorded in situ. Proceedings of the National Academy of Sciences of the USA 109:7169–7174.

Kareiva, P., and G. Odell. 1987. Swarms of predators exhibit "preytaxis" if individual predators use area-restricted search. American Naturalist 130:233–270.

Krebs, J. R., J. T. Erichsen, M. I. Webber, and E. L. Charnov. 1977. Optimal prey selection in the great tit (*Parus major*). Animal Behaviour 25:30–38.

Kölzsch, A., A. Alzate, F. Bartumeus, M. de Jager, E. J. Weerman, G. M. Hengeveld, M. Naguib, B. A. Nolet, and J. van de Koppel. 2015. Experimental evidence for inherent Lévy search behaviour in foraging animals. Proceedings of the Royal Society B 282:20150424.

Levernier, N., O. Bénichou, and R. Voituriez. 2021. Universality classes of hitting probabilities of jump processes. Physical Review Letters 126:100602.

Lihoreau, M., T. C. Ings, L. Chittka, and A. M. Reynolds. 2016. Signatures of a globally optimal searching strategy in the three-dimensional foraging flights of bumblebees. Scientific Reports 6:30401.

Liu, Y., X. Long, P. Martin, S. Solomon, and P. Gong. 2021. Lévy walk dynamics explain gamma burst patterns in primate cerebral cortex. Communications Biology 4:739.

Loken, C., D. Gruner, L. Groer, R. Peltier, N. Bunn, M. Craig, T. Henriques, et al. 2010. SciNet: lessons learned from building a power-efficient top-20 system and data centre. Journal of Physics: Conference Series 256:012026.

López-Incera, A., K. Ried, T. Müller, and H. J. Briegel. 2020. Development of swarm behavior in artificial learning agents that adapt to different foraging environments. PLoS ONE 15:e0243628.

McKerns, M. M., L. Strand, T. Sullivan, A. Fang, and M. A. G. Aivazis. 2012. Building a framework for predictive science. arXiv, https://doi.org/10.48550/arXiv.1202.1056.

McKinney, W. 2010. Data structures for statistical computing in Python. Pages 56–61 *in* Stéfan van der Walt and Jarrod Millman, eds. Proceedings of the 9th Python in Science Conference.

Meire, P., and A. Ervynck. 1986. Are oystercatchers (*Haematopus ostralegus*) selecting the most profitable mussels (*Mytilus edulis*)? Animal Behaviour 34:1427–1435.

Miramontes, O., O. DeSouza, L. R. Paiva, A. Marins, and S. Orozco. 2014. Lévy flights and self-similar exploratory behaviour of termite workers: beyond model fitting. PLoS ONE 9:e111183.

Murakami, H., T. Niizato, T. Tomaru, Y. Nishiyama, and Y.-P. Gunji. 2015. Inherent noise appears as a Lévy walk in fish schools. Scientific Reports 5:10605.

Pacheco-Cobos, L., B. Winterhalder, C. Cuatianquiz Lima, M. Rosetti, R. Hudson, and C. Ross. 2019. Nahua mushroom gatherers use area-restricted search strategies that conform to marginal value theorem predictions. Proceedings of the National Academy of Sciences of the USA 116:201814476.

Ponce, M., R. van Zon, S. Northrup, D. Gruner, J. Chen, F. Ertinaz, A. Fedoseev, et al. 2019. Deploying a top-100 supercomputer for large parallel workloads: the Niagara supercomputer. *In* Proceedings of the Practice and Experience in Advanced Research Computing on Rise of the Machines (Learning). PEARC'19. Association for Computing Machinery, New York.

Raichlen, D. A., B. M. Wood, A. D. Gordon, A. Z. P. Mabulla, F. W. Marlowe, and H. Pontzer. 2014. Evidence of Lévy walk foraging patterns in human hunter–gatherers. Proceedings of the National Academy of Sciences of the USA 111:728–733.

Ramos-Fernandez, G., J. Mateos, O. Miramontes, C. Germinal, H. Larralde, and B. Ayala-Orozco. 2004. Lévy walk patterns in the foraging movements of spider monkeys (*Ateles geoffroyi*). Behavioral Ecology and Sociobiology 55:223–230.

Reijers, V. C., K. Siteur, S. Hoeks, J. van Belzen, A. C. W. Borst, J. H. T. Heusinkveld, L. L. Govers, et al. 2019. A Lévy expansion strategy optimizes early dune building by beach grasses. Nature Communications 10:2656.

Reynolds, A., E. Ceccon, C. Baldauf, T. Karina Medeiros, and O. Miramontes. 2018. Lévy foraging patterns of rural humans. PLoS ONE 13:e0199099.

Reynolds, A. M. 2018. Current status and future directions of Lévy walk research. Biology Open 7:bio030106.

———. 2021. Weierstrassian Lévy walks are a by-product of crawling. European Physical Journal E 44:96.

Reynolds, A. M., and M. A. Frye. 2007. Free-flight odor tracking in *Drosophila* is consistent with an optimal intermittent scale-free search. PLoS ONE 2:e354.

Scharf, I., B. Kotler, and O. Ovadia. 2009. Consequences of food distribution for optimal searching behavior: an evolutionary model. Evolutionary Ecology 23:245–259.

Shirakawa, T., T. Niizato, H. Sato, and R. Ohno. 2019. Biased Lévy-walk pattern in the exploratory behavior of the *Physarum* plasmodium. Biosystems 182:52–58.

Sims, D. W., N. E. Humphries, N. Hu, V. Medan, and J. Berni. 2019. Optimal searching behaviour generated intrinsically by the central pattern generator for locomotion. eLife 8:e50316.

Sims, D. W., A. M. Reynolds, N. E. Humphries, E. J. Southall, V. J. Wearmouth, B. Metcalfe, and R. J. Twitchett. 2014. Hierarchical random walks in trace fossils and the origin of optimal search behavior. Proceedings of the National Academy of Sciences of the USA 111:11073–11078.

Sims, D. W., E. J. Southall, N. E. Humphries, G. C. Hays, C. J. A. Bradshaw, J. W. Pitchford, A. James, et al. 2008. Scaling laws of marine predator search behaviour. Nature 451:1098–1102.

Sloss, A. N., and S. Gustafson. 2020. 2019 evolutionary algorithms review. Pages 307–344 *in* Genetic programming theory and practice XVII. Springer, Cham.

Tromp, J. 2016. The number of legal go positions. Pages 183–190 *in* Computers and games. Springer, Cham.

Virtanen, P., R. Gommers, T. E. Oliphant, M. Haberland, T. Reddy, D. Cournapeau, E. Burovski, et al. 2020. Scipy 1.0: fundamental algorithms for scientific computing in python. Nature Methods 17:261–272.

Viswanathan, G., S. Buldyrev, S. Havlin, M. Luz, E. P. Raposo, and H. Stanley. 1999. Optimizing the success of random searches. Nature 401:911–914.

Viswanathan, G., E. Raposo, and M. da Luz. 2008. Lévy flights and superdiffusion in the context of biological encounters and random searches. Physics of Life Reviews 5:133–150.

Walraet, M., and J. Tromp. 2016. A googolplex of go games. Pages 191–201 *in* Computers and games. Springer, Cham.

Werner, E. E., and D. J. Hall. 1974. Optimal foraging and the size selection of prey by the bluegill sunfish (*Lepomis macrochirus*). Ecology 55:1042–1052.

Wiser, M. J., and R. E. Lenski. 2015. A comparison of methods to measure fitness in *Escherichia coli*. PLoS ONE 10:e0126210.

Wosniack, M. E., M. C. Santos, E. P. Raposo, G. M. Viswanathan, and M. G. E. da Luz. 2017. The evolutionary origins of Lévy walk foraging. PLoS Computational Biology 13:e1005774.

Zhou, H., S. Yang, and S. Zhang. 2018. Conformable derivative approach to anomalous diffusion. Physica A 491:1001–1013.

Associate Editor: Éva Kisdi
Editor: Erol Akçay

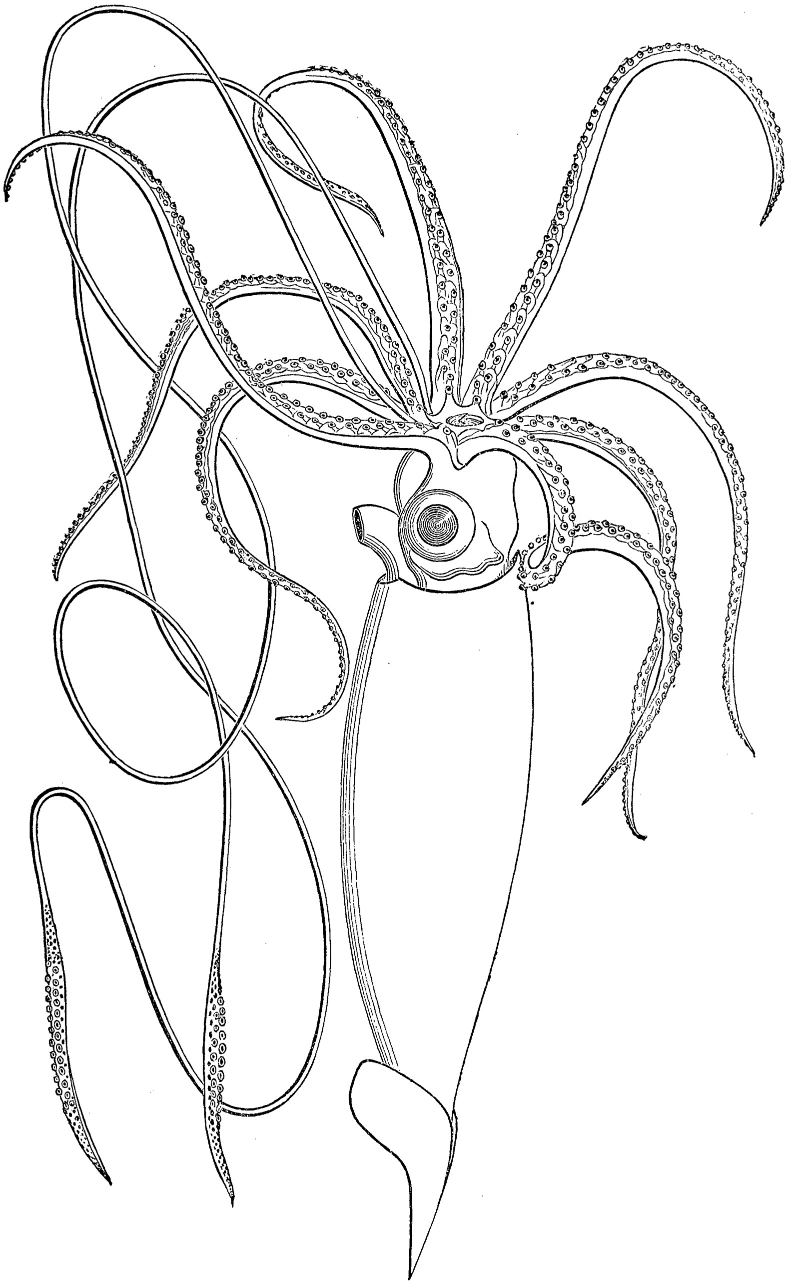

"Architeuthis monachus (No. 5), one twenty-second natural size, from Logie Bay, N. F." From "The Colossal Cephalopods of the North Atlantic" by A. E. Verrill (*The American Naturalist*, 1875, 9:21–36).